New Journal of Physics
The open access journal at the forefront of physics

Deutsche Physikalische Gesellschaft DPG IOP Institute of Physics

OPEN ACCESS

Reflection of a Lieb–Liniger wave packet from the hard-wall potential

To cite this article: D Jukić and H Buljan 2010 *New J. Phys.* **12** 055010

View the article online for updates and enhancements.

You may also like

- Non relativistic limit of integrable QFT and Lieb–Liniger models
Alvise Bastianello, Andrea De Luca and Giuseppe Mussardo

- Generalized hydrodynamics in the one-dimensional Bose gas: theory and experiments
Isabelle Bouchoule and Jérôme Dubail

- A coordinate Bethe ansatz approach to the calculation of equilibrium and nonequilibrium correlations of the one-dimensional Bose gas
Jan C Zill, Tod M Wright, Karén V Kheruntsyan et al.

This content was downloaded from IP address 3.142.198.129 on 27/04/2024 at 04:18

New Journal of Physics
The open-access journal for physics

Reflection of a Lieb–Liniger wave packet from the hard-wall potential

D Jukić and H Buljan[1]
Department of Physics, University of Zagreb, Bijenička c. 32, 10000 Zagreb, Croatia
E-mail: hbuljan@phy.hr

New Journal of Physics **12** (2010) 055010 (15pp)
Received 2 November 2009
Published 28 May 2010
Online at http://www.njp.org/
doi:10.1088/1367-2630/12/5/055010

Abstract. Non-equilibrium dynamics of a Lieb–Liniger system in the presence of the hard-wall potential is studied. We demonstrate that a time-dependent wave function, which describes quantum dynamics of a Lieb–Liniger wave packet consisting of N particles, can be found by solving an N-dimensional Fourier transform; this follows from the symmetry properties of the many-body eigenstates in the presence of the hard-wall potential. The presented formalism is employed to numerically calculate reflection of a few-body wave packet from the hard wall for various interaction strengths and incident momenta.

Contents

1. Introduction **2**
2. Eigenstates in the presence of the hard-wall potential **4**
3. Many-body dynamics in time via a Fourier transform **5**
4. Example: a Lieb–Liniger wave packet incident on the hard wall **8**
4.1. Normalization of eigenstates 12
4.2. Connection to physical units 13
5. Conclusion **13**
Acknowledgments **13**
Appendix. The ground state of a Lieb–Liniger gas in an infinitely deep box **13**
References **14**

[1] Author to whom any correspondence should be addressed.

© IOP Publishing Ltd and Deutsche Physikalische Gesellschaft

1. Introduction

Recent intensive theoretical studies of one-dimensional (1D) Bose gases have been motivated mainly by the experimental realizations [1]–[5] of the models [6, 7] describing these systems. Ultracold atomic gases in tight atomic wave guides can have their transversal degrees of freedom essentially frozen such that their motion becomes effectively 1D [1]–[5]. These systems are described in terms of the Lieb–Liniger model, i.e. a system of identical Bose particles in 1D with point-like δ-function interactions of arbitrary strength c [6]. In the limit of strong coupling ($c \to \infty$), the Lieb–Liniger gas approaches the Tonks–Girardeau (TG) regime of impenetrable bosons [7], which has been experimentally achieved as well [2]; the TG regime occurs at very low temperatures, low linear densities, and with strong effective interactions [8]–[10]. Experiments are even capable of exploring non-equilibrium quantum dynamics of these 1D many-body systems [3, 4], which may occur after some sudden change in the system's parameters. These ultracold atomic assemblies are well isolated from the environment, that is, their quantum coherence stays preserved for long times. Therefore, they may serve as a playground to investigate relaxation of isolated quantum many-body systems, which is one of the most interesting questions in theoretical physics (e.g. see [11]–[18] and references therein). Subsequent relaxation of 1D gases via collisions is greatly determined by the reduced dimensionality and the integrability of the underlying models. We are motivated to study the time-dependent Lieb–Liniger model because (i) today's experiments can explore fundamental physical questions in these systems [3, 4] and (ii) one can construct exact solutions of some relevant problems for all interaction strengths (from the mean field regime up to the strongly correlated regime) [19]–[24].

The eigenstates of the Lieb–Liniger model (without an external potential present), which were constructed by employing the Bethe ansatz [6], are determined by a set of quasi-momenta; when periodic [6] boundary conditions are imposed, the quasi-momenta must obey a set of transcendental Bethe equations [6]. The Lieb–Liniger eigenstates in the presence of the hard wall (i.e. on the semi-infinite line) can be constructed via superposition of free space eigenstates [25]; again, if the quasi-momenta should obey a particular set of transcendental equations [25], this superposition yields eigenstates in an infinitely deep box [25]. Recent years have witnessed an increasing interest in exact solutions of these models (e.g. see [26]–[32] and references therein), most of which are focused on the properties of the ground and excited eigenstates (see also [33, 34]). Unfortunately, the Lieb–Liniger model does not reveal exact solutions in the presence of some smooth external trapping potential $V(x)$ (e.g. the harmonic potential).

In the TG limit $c \to \infty$, the methods for finding eigenstates [7], time-dependent solutions [35], as well as observables (see, e.g., [36] for the system of hard-core bosons on the lattice and [37] for the continuous TG model) are much simpler due to the Fermi–Bose mapping, which in a simple fashion maps a fermionic wave function describing spinless non-interacting fermions onto a TG wave function [7, 35]. It is important to emphasize that these methods are valid for any external potential. Perhaps the simplicity of the methods and phenomenological relevance of the model [3] have led to increasing interest in quantum many-body dynamics of TG gases. Some of these studies include dynamics during free expansion [36], [38]–[40], dynamics of dark soliton-like states [35] and reflections from a periodic potential [37].

In the case of finite interaction strength c, it is far more difficult to calculate exact many-body wave functions and/or observables describing dynamics of time-dependent Lieb–Liniger

wave packets. Without attempting to provide a review, let us mention a few approaches utilized to study non-equilibrium dynamics of 1D interacting Bose gases. The hydrodynamic formalism [10] (the local density approximation) can be formulated in terms of the nonlinear Schrödinger-like equation with variable nonlinearity [41]; this approach reduces to the Gross–Pitaevskii theory in the weakly interacting limit [10, 41]. More sophisticated numerical approaches include the time-evolving block decimation algorithm [42], which has recently been utilized to study relaxation following a quench in a 1D Bose gas [43], the two-particle irreducible (2PI) effective action approach [44, 45], the multi-configurational time-dependent Hartree method for bosons (MCTDHB) [46] (the MCTDHB method is numerically exact when sufficiently many time-dependent orbitals are taken into account), and the multi-configurational time-dependent Hartree method (e.g. see [47] and references therein). Gritsev *et al* [24] provide a discussion of several methods that can be used to describe non-equilibrium dynamics of Lieb–Liniger gases with a greater focus on the form-factor approach [24], which has been recently utilized to calculate equilibrium correlation functions of a 1D Bose gas (see [48] and references therein). A broader review discussing many-body physics with ultracold gases can be found in [49]. We also mention a recent review on quantum transients [50].

An interesting exact method was outlined by Gaudin way back in 1983 [19]: a time-dependent Lieb–Liniger wave function on an infinite line, in the absence of an external potential, can be constructed by acting with a differential operator (which contains the interaction strength parameter c) onto a time-dependent wave function describing non-interacting (spin polarized) 1D fermions [19], [21]–[23], [51]. For dynamics of a Lieb–Liniger wave packet consisting of N particles, this method reduces to finding an N-dimensional Fourier transform, which can be used to extract the asymptotic behavior of the wave function and some observables during the course of 1D free expansion [22, 23]. In this article, we investigate the possibility of extending this approach to study the dynamics of a Lieb–Liniger wave packet in the presence of the hard-wall potential.

Our interest in quantum dynamics in the presence of the hard-wall potential is in part motivated by experiments. More specifically, the interaction of Bose–Einstein condensates (BECs) with surfaces is of interest for the implementation of atom interferometry on chips [52]. A BEC falling under gravity, and then reflecting from a light sheet, has been experimentally and theoretically studied in [53]. Moreover, one of the prominent experimental activities nowadays is deceleration of atomic beams by reflection from a moving mirror. This work first started with neutrons being cooled by reflecting from a moving Ni surface [54]. In cold atom physics, there have been several experiments for manipulation and slowing down of atomic beams with the use of reflection in mirrors [55]–[57].

Here we explore, by using exact methods, the dynamics of Lieb–Liniger wave packets in the presence of the hard-wall potential, more specifically, reflection of a Lieb–Liniger wave packet from such a wall. The outline of the paper is as follows. In section 2, we introduce the model and outline the construction of eigenstates in the given external potential. In section 3, we analytically discuss time-dependent quantum dynamics of the system that starts from a general initial condition. By employing the symmetries of the Lieb–Liniger eigenstates, we demonstrate that a time-dependent Lieb–Liniger wave packet reflecting from the wall can be calculated by solving an N-dimensional Fourier transform, where N is the number of particles. This opens the way to calculate the asymptotic properties of the wave packet by employing the stationary phase approximation as in [22, 23] for free expansion. In section 4, we utilize the formalism to numerically study the dynamics of single-particle (SP) density and momentum distribution

of a few-body wave packet reflecting from the wall. We find that the wave packets for smaller interaction strength c get reflected at a slower rate. The interference fringes that occur during the dynamics have larger visibility for smaller values of c.

2. Eigenstates in the presence of the hard-wall potential

The Lieb–Liniger model describes N identical bosons in one spatial dimension, which interact via a repulsive δ-function potential of strength $c > 0$. The model can be represented in terms of the Schrödinger equation:

$$\mathrm{i}\frac{\partial\psi}{\partial t} = -\sum_{i=1}^{N}\frac{\partial^2\psi}{\partial x_i^2} + \sum_{1\leqslant i<j\leqslant N} 2c\,\delta(x_i - x_j)\psi + \sum_{i=1}^{N} V(x_i)\psi(x_1,\ldots,x_N,t). \tag{1}$$

As we have already stated, this model can be experimentally realized with ultracold atoms in tight atomic waveguides. The spatial and temporal coordinates (x and t, respectively), as well as the potential $V(x)$ are dimensionless in this paper. Their connection to physical units is as follows: $x = X/X_0$, $t = T/T_0$ and $V(x) = U(X)/E_0$, where X, T and $U(X)$ are space, time and energy variables in physical units. Given the mass of the atoms m, the choice of an arbitrary length scale X_0 sets the time scale $T_0 = 2mX_0^2/\hbar$ and energy scale $E_0 = \hbar^2/(2mX_0^2)$. Suppose that the transverse confinement of the atomic waveguide is described by a harmonic oscillator with frequency $\omega_\perp$. The interaction parameter c is proportional to the effective 1D coupling strength $g_{1\mathrm{D}}$ [8], $2c = g_{1\mathrm{D}}/(X_0E_0) = g_{1\mathrm{D}}\,2mX_0/\hbar^2$, which is related to the 1D scattering length $a_{1\mathrm{D}}$ via $g_{1\mathrm{D}} = -2\hbar^2/ma_{1\mathrm{D}}$; the 1D scattering length $a_{1\mathrm{D}} = -(l_\perp^2/a)(1 - Ca/\sqrt{2}l_\perp)$ depends on three-dimensional scattering length a and the transverse oscillator width $l_\perp = \sqrt{\hbar/m\omega_\perp}$ (the constant $C = 1.4603\ldots$).

In the present paper, we focus on the dynamics (in time) of a Lieb–Liniger wave packet in the presence of the hard-wall potential, that is,

$$V(x) = \begin{cases} 0, & \text{if } x > 0 \\ \infty, & \text{if } x \leqslant 0. \end{cases} \tag{2}$$

We will show that the solution of this problem can be constructed by solving an N-dimensional Fourier transform. To this end, we need eigenstates of a Lieb–Liniger gas in the hard-wall potential. First, let us write down the Lieb–Liniger eigenstates in free space (i.e. $x \in (-\infty, \infty)$ without external potentials and any boundary conditions) [6, 33]:

$$\begin{aligned}\psi_{\{k\}} &= \mathcal{N}(\{k\})\sum_P(-1)^P\prod_{i<j}\left[\mathrm{sgn}(x_j - x_i) + \frac{\mathrm{i}}{c}(k_{Pj} - k_{Pi})\right]\mathrm{e}^{\mathrm{i}\sum_j k_{Pj}x_j} \\ &= \mathcal{N}(\{k\})\sum_P(-1)^P a(P,\{k\})\mathrm{e}^{\mathrm{i}\sum_j k_{Pj}x_j},\end{aligned} \tag{3}$$

where $\{k\} = \{k_m \,|\, m = 1,\ldots,N\}$ is a set of (real) distinct quasi-momenta, which uniquely determine the eigenstate, P denotes a permutation of N numbers, $P \in S_N$, and we have implicitly defined $a(P,\{k\})$. The normalization of these eigenstates is given by [33, 34]

$$\frac{1}{\mathcal{N}(\{k\})} = \sqrt{N!(2\pi)^N\prod_{i<j}\left[1 + \left(\frac{k_j - k_i}{c}\right)^2\right]},$$

that is, within the fundamental sector in k-space, $k_1 < \cdots < k_N$ and $k'_1 < \cdots < k'_N$, we have

$$\int_{-\infty}^{\infty} \psi^*_{\{k\}} \psi_{\{k'\}} \mathrm{d}x_1 \cdots \mathrm{d}x_N = \prod_{j=1}^{N} \delta(k_j - k'_j). \tag{4}$$

The Lieb–Liniger eigenstates in the presence of the hard wall (denoted by $\phi_{\{k\}}$) were first constructed by Gaudin [25] as a superposition of 2^N free-space eigenstates. This superposition obeys the hard-wall boundary condition: $\phi_{\{k\}}(x_1 = 0, x_2, \ldots, x_N) = 0$ in the fundamental sector $R_1 : x_1 < x_2 < \cdots < x_N$ of x-space. These eigenstates are expressed as follows:

$$\phi_{\{k\}} = \sum_{\{\epsilon\}} A(\{\epsilon\}, \{k\}) \psi_{\{\epsilon k\}}, \tag{5}$$

where $\{\epsilon\} = \{\epsilon_m | \epsilon_m \in \{-1, 1\}, m = 1, \ldots, N\}$ and $\{\epsilon k\} = \{\epsilon_m k_m \,|\, \epsilon_m \in \{-1, 1\}, m = 1, \ldots, N\}$; evidently, there are 2^N such sets and therefore 2^N terms in the sum (5). The quantity $A(\{\epsilon\}, \{k\})$ is defined by

$$A(\{\epsilon\}, \{k\}) = \epsilon_1 \cdots \epsilon_N \; A'(\epsilon_1 k_1, \epsilon_2 k_2, \ldots, \epsilon_N k_N), \tag{6}$$

where

$$A'(k_1, k_2, \ldots, k_N) \equiv \frac{\prod_{i<j} \left[1 + \frac{\mathrm{i}}{c}(k_j + k_i)\right]}{\sqrt{\prod_{i<j} \left[1 + \left(\frac{k_j + k_i}{c}\right)^2\right]}} \tag{7}$$

are the coefficients utilized in the superposition. It is straightforward to verify that indeed $\phi_{\{k\}}(x_1 = 0, x_2, \ldots, x_N) = 0$ in the fundamental sector R_1 [25].

However, it is not simple to prove that these eigenstates are orthogonal and normalized. This is of key importance if one wishes to project some initial state onto these eigenstates and calculate time-evolution in the standard fashion via superposition over eigenstates. In section 4, we discuss the normalization of eigenstates (5) and, based on our numerical investigations, conjecture that these eigenstates are orthogonal and normalized.

3. Many-body dynamics in time via a Fourier transform

In this section, we demonstrate that a solution of the time-dependent equation (1) with the hard-wall potential (2) can be expressed in terms of an N-dimensional Fourier transform. We assume that at time $t = 0$ the wave packet is localized in the vicinity of the wall. For example, the initial state ψ_0 can be the ground state wave function in some external trapping potential; if at $t = 0$ this potential is suddenly turned off, the wave packet will start expanding and some of its components will be reflected from the wall, which will give rise to interference effects. Such a scenario is possible to create with today's experimental capabilities [3]. One possible (similar) scenario is as follows: suppose that at $t = 0$ the aforementioned trapping potential is turned off, and that in the next instance the many body wave packet is given some momentum kick, say toward the wall; the reflection and interference phenomena will depend on the interactions and imparted momentum. During the reflection, particles will collide and one may ask to what extent will the initial conditions be forgotten (or blurred) after the reflection?

To describe quantum dynamics from the initial conditions described above, we write the initial state ψ_0 as a superposition over a complete set of eigenstates $\phi_{\{k\}}$:

$$\psi_0 = \int_{0<k_1<\cdots<k_N} b(k_1, \ldots, k_N)\phi_{\{k\}} \mathrm{d}k_1 \ldots \mathrm{d}k_N. \tag{8}$$

The subsequent derivation is based on the following two relations obeyed by the eigenstates $\phi_{\{k\}}$:

$$\phi_{\{k\}} = (-1)^P \phi_{\{Pk\}} \tag{9}$$

and

$$\phi_{\{k\}} = -\phi_{\{k_1,\ldots,k_{j-1},-k_j,k_{j+1}\ldots,k_N\}}. \tag{10}$$

Equation (9) follows from the definition of $\phi_{\{k\}}$ in equation (5), and the fact that the Lieb–Liniger eigenstates in free space $\psi_{\{k\}}$ obey an identical relation: $\psi_{\{k\}} = (-1)^P \psi_{\{Pk\}}$; this identity can be traced to the fact that $\psi_{\{k\}}$ are antisymmetric with respect to the interchange of any two variables k_i and k_j [33]. The derivation of equation (10) is straightforward. Let us define a set $\{\epsilon'\}$, which corresponds to the set $\{\epsilon\}$ as follows: $\{\epsilon'_1, \ldots, \epsilon'_N\} = \{\epsilon_1, \ldots, \epsilon_{j-1}, -\epsilon_j, \epsilon_{j+1}, \ldots, \epsilon_N\}$; it is evident from the definition (5) that $\phi_{\{k\}} = \sum_{\{\epsilon'\}} A(\{\epsilon'\}, \{k\})\psi_{\{\epsilon' k\}}$. Furthermore, let us denote $\{k'\} = \{k_1, \ldots, k_{j-1}, -k_j, k_{j+1} \ldots, k_N\}$, i.e. the set of k-values $\{k'\}$ is identical to the set $\{k\}$ except that k_j is reversed in sign. By using $A(\{\epsilon\}, \{k\}) = -A(\{\epsilon'\}, \{k'\})$ and $\{\epsilon' k'\} = \{\epsilon k\}$, we have

$$\phi_{\{k'\}} = \sum_{\{\epsilon'\}} A(\{\epsilon'\}, \{k'\})\psi_{\{\epsilon' k'\}} = -\sum_{\{\epsilon\}} A(\{\epsilon\}, \{k\})\psi_{\{\epsilon k\}} = -\phi_{\{k\}}, \tag{11}$$

that is, we obtain equation (10). We note in passing that if any $k_j = 0$, then $\phi_{\{k\}} = 0$, which follows from equation (10); furthermore, $\phi_{\{k\}}$ is also zero whenever any two of the quasi-momenta k_i and k_j are equal.

Due to the symmetry of the hard-wall eigenstates $\phi_{\{k\}}$ presented in equations (9) and (10), a complete set of eigenstates is spanned in the region of the k-space defined by $0 < k_1 < \cdots < k_N$, which we will refer to as the fundamental region in k-space, and denote it with Q_1^+. Hence, the integral in equation (8) spans over Q_1^+. Furthermore, by employing relations (9) and (10), ψ_0 can be written as an integral over the whole k-space:

$$\psi_0 = \int_{-\infty}^{\infty} \mathrm{d}k_1 \cdots \mathrm{d}k_N G(k_1, \ldots, k_N) \exp\left(\mathrm{i}\sum_j k_j x_j\right), \tag{12}$$

where the function G is defined as

$$G(k_1, \ldots, k_N) = b(k_1, \ldots, k_N) A'(k_1, \ldots, k_N) \mathcal{N}(\{k\}) \prod_{i<j} \left[\mathrm{sgn}(x_j - x_i) + \frac{\mathrm{i}}{c}(k_j - k_i)\right]. \tag{13}$$

From equation (13) it immediately follows that the time evolution of a Lieb–Liniger wave packet in the presence of the hard wall can be calculated from an N-dimensional Fourier transform.

In order to derive equations (12) and (13), first note that due to (9) and (10), the projection coefficients satisfy

$$b(k_1, \ldots, k_N) = (-1)^P b(k_{P1}, \ldots, k_{PN}) \tag{14}$$

and

$$b(k_1, \ldots, k_N) = -b(k_1, \ldots, k_{j-1}, -k_j, k_{j+1}, \ldots, k_N), \tag{15}$$

the latter identity can conveniently be rewritten as

$$b(k_1, \ldots, k_N) = \epsilon_1 \cdots \epsilon_N b(\epsilon_1 k_1, \ldots, \epsilon_N k_N). \tag{16}$$

By employing the symmetries of the Lieb–Liniger hard-wall eigenstates, which are inherited by the expansion coefficients $b(k_1, \ldots, k_N)$, equation (8) can be rewritten as follows:

$$\psi_0 = \frac{1}{N!} \int_{k_1>0,\ldots,k_N>0} \mathrm{d}k_1 \cdots \mathrm{d}k_N b(k_1, \ldots, k_N) \sum_{\{\epsilon\}} A(\{\epsilon\}, \{k\}) \times \mathcal{N}(\epsilon_1 k_1, \ldots, \epsilon_N k_N) \sum_P (-1)^P a(P, \{\epsilon k\}) \exp\left(\mathrm{i} \sum_j \epsilon_{Pj} k_{Pj} x_j\right) \tag{17}$$

$$= \frac{1}{N!} \int_{k_1>0,\ldots,k_N>0} \mathrm{d}k_1 \cdots \mathrm{d}k_N \sum_{\{\epsilon\}} b(\epsilon_1 k_1, \ldots, \epsilon_N k_N) A'(\epsilon_1 k_1, \ldots, \epsilon_N k_N) \times \mathcal{N}(\epsilon_1 k_1, \ldots, \epsilon_N k_N) \sum_P (-1)^P a(P, \{\epsilon k\}) \exp\left(\mathrm{i} \sum_j \epsilon_{Pj} k_{Pj} x_j\right) \tag{18}$$

$$= \frac{1}{N!} \int_{-\infty}^{\infty} \mathrm{d}k_1 \cdots \mathrm{d}k_N\, b(k_1, \ldots, k_N) A'(k_1, \ldots, k_N) \times \mathcal{N}(k_1, \ldots, k_N) \sum_P (-1)^P a(P, \{k\}) \exp\left(\mathrm{i} \sum_j k_{Pj} x_j\right) \tag{19}$$

$$= \frac{1}{N!} \sum_P \int_{-\infty}^{\infty} \mathrm{d}k_1 \cdots \mathrm{d}k_N\, b(k_{P1}, \ldots, k_{PN}) A'(k_{P1}, \ldots, k_{PN}) \times \mathcal{N}(k_{P1}, \ldots, k_{PN}) a(P, \{k\}) \exp\left(\mathrm{i} \sum_j k_{Pj} x_j\right) \tag{20}$$

$$= \frac{1}{N!} \sum_P \int_{-\infty}^{\infty} \mathrm{d}k_{P1} \cdots \mathrm{d}k_{PN}\, b(k_{P1}, \ldots, k_{PN}) A'(k_{P1}, \ldots, k_{PN}) \times \mathcal{N}(k_{P1}, \ldots, k_{PN}) a(P, \{k\}) \exp\left(\mathrm{i} \sum_j k_{Pj} x_j\right), \tag{21}$$

from which we immediately obtain equations (12) and (13) because the sum over all permutations P is a sum over $N!$ identical integrals. In the above derivation, the first identity, equation (17), follows from the properties (9) and (14). The second identity (18) is due to (16) and the definition of $A(\{\epsilon\}, \{k\})$ in equation (6). By employing equations (10) and (16), the sum over $\{\epsilon\}$ in equation (18) can be replaced by integrating over the whole k-space to obtain the third equality, equation (19). By using identities $A'(k_{P1}, \ldots, k_{PN}) = A'(k_1, \ldots, k_N)$ and $\mathcal{N}(k_{P1}, \ldots, k_{PN}) = \mathcal{N}(k_1, \ldots, k_N)$, together with equation (14), we obtain (20).

The time-dependent solution of the many-body Schrödinger equation (1) with $V(x)$ given by (2) is simply

$$\psi = \int_{-\infty}^{\infty} \mathrm{d}k_1 \ldots \mathrm{d}k_N G(k_1, \ldots, k_N) \exp\left(\mathrm{i} \sum_j (k_j x_j - k_j^2 t)\right). \tag{22}$$

Thus, by knowing the function G that contains all information about the initial condition and that is simply related to the projection coefficients $b(k_1, \ldots, k_N)$ of the initial state onto hard-wall Lieb–Liniger eigenstates $\phi_{\{k\}}$, we can compute the time-dependent Lieb–Liniger wave function in the hard-wall potential by employing the Fourier transform. With this identification, an exact analysis of this many-body problem is at least conceptually considerably simplified.

We note that the asymptotic behavior of the many-body state and the observables such as SP density or momentum distribution can be straightforwardly extracted from expression (22) by using the stationary phase approximation, as was done in [22, 23] for the case of free expansion of a Lieb–Liniger gas (see, e.g., equation (15) in [22], and equations (18) and (19) in [23]). From these methods, and equations (22) and (13), it follows that the initial conditions are imprinted into asymptotic states. It is straightforward to infer that the asymptotic wave functions, $\psi_\infty(\eta_1, \ldots, \eta_N, t) = \psi(\eta_1 t, \ldots, \eta_N t, t)$ for sufficiently large t, vanish at the hyperplanes of contact between particles $\eta_i = \eta_j$ $(i \neq j)$, which is characteristic for TG wave functions [7]. However, it should be emphasized that the properties of such asymptotic states can considerably differ from the physical properties of a TG gas in the ground state of some trapping potential [22] (see also the second item of [21]). Moreover, the asymptotic momentum distribution coincides, up to a simple scaling transformation, with the shape of the asymptotic SP density in x-space, reflecting the fact that the dynamics is asymptotically ballistic [23]; this means that at asymptotic times, despite the fact that the wave functions have attained the TG structure, interactions do not affect the dynamics any more. From the connection between the asymptotic momentum distribution and SP density one finds that the asymptotic momentum distribution is zero at $k = 0$, and it is located on the positive k-axis, which simply means that for sufficiently large times the particles move away from the wall.

4. Example: a Lieb–Liniger wave packet incident on the hard wall

In this section, we study a specific example of a localized Lieb–Liniger wave packet consisting of $N = 3$ particles reflecting from the hard-wall potential. More specifically, we assume that for $t < 0$ the Lieb–Liniger system is in the ground state of an infinitely deep box denoted by $\psi_{g.s.}(x_1, x_2, x_3)$. The analytic expression for this ground state was found in [25]; for reasons of completeness, in the appendix, we present its construction. In our simulations, the box is in the interval $[1.5\pi, 2.5\pi]$, i.e. $\psi_{g.s.}(x_1, x_2, x_3)$ is zero whenever any x_i is outside this interval. At $t = 0$, the box potential is suddenly turned off, and the wave packet is simultaneously (and suddenly) imparted some momentum of magnitude $K \geqslant 0$ toward the wall: $\psi(x_1, x_2, x_3, t = 0) = \psi_{g.s.}(x_1, x_2, x_3)\exp[-\mathrm{i}K(x_1 + x_2 + x_3)]$; apparently, K denotes the imparted momentum per particle. From such an initial state, we are able to find projection coefficients $b(k_1, k_2, k_3)$ defined in equation (8), that is, we can find the corresponding function $G(k_1, k_2, k_3)$, which is needed to calculate the Fourier transform (22). The Fourier integral in (22) is in this particular example three-dimensional, and it is calculated numerically by using the fast Fourier transform algorithm in MATLAB. This provides us with the time-dependent

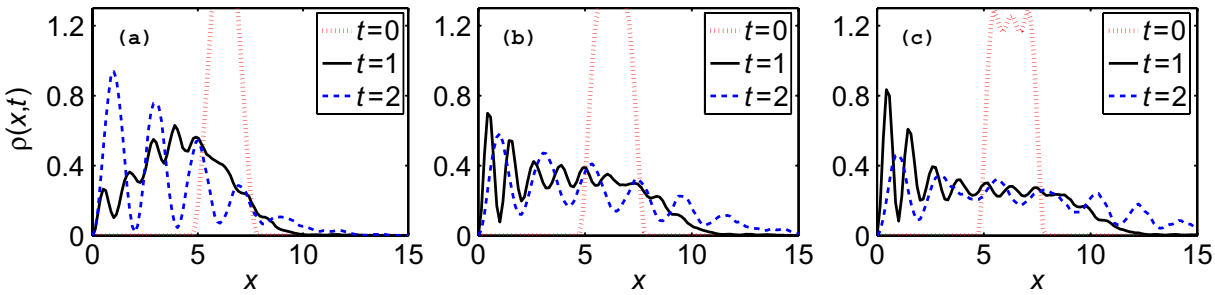

Figure 1. Density evolution of a Lieb–Liniger wave packet consisting of $N = 3$ bosons, which is given some momentum kick K (per particle) toward the wall. Insets correspond to the interaction strengths (a) $c = 0.25$, (b) $c = 3$ and (c) $c = 10$. The imparted momentum is $K = 1$. Red dotted lines are for $t = 0$, black solid lines are for $t = 1$ and blue dashed lines are for $t = 2$.

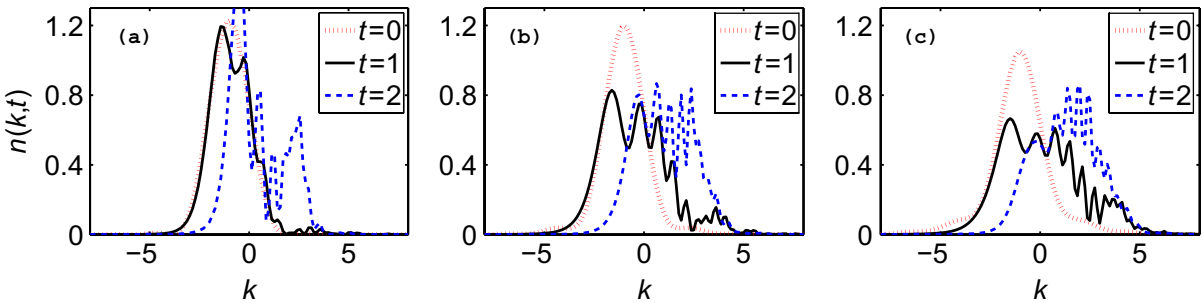

Figure 2. The same as figure 1 but for the momentum distribution.

wave function $\psi(x_1, x_2, x_3, t)$, which we use to study the dynamics of observables such as the SP density $\rho(x, t)$ or the momentum distribution $n(k, t)$.

First, let us explore the effect of the interactions on the reflections of a few-body Lieb–Liniger wave packet. In figures 1 and 2, we plot the time evolution of SP densities and distributions of the momenta, respectively. The plots are made at three different times, $t = 0$, 1 and 2, and for three values of the coupling parameter, $c = 0.25$, 3 and 10. The magnitude of the imparted momentum per particle is $K = 1$. Note that the wave packets broaden in time due to the repulsive interactions between the particles, and also due to the wave dispersion effects; the wave packets for larger values of c spread at a faster rate than the wave packets for smaller c. From figures 1 and 2, we observe that wave packets with a larger interaction parameter c get reflected faster than the wave packets for smaller c; for wave packets with smaller repulsion between the particles (smaller c), the compression of the wave packet is stronger, and therefore reflection of the momenta occurs at a slower rate. We also observe that all wave packets exhibit interference fringes during the reflection process. However, we find the interference fringes to be deeper for smaller values of c, which follows from the fact that the wave packets for smaller c are more spatially coherent. This can also be seen in figure 2, which displays momentum distributions. The distribution $n(k, t)$ for $c = 0.25$, at the largest time shown $t = 2$, has one strong well-defined peak (the one closest to zero), and several smaller peaks of the wave components with larger magnitude of the momentum (see figure 2(a)). In contrast, for $c = 10$ this most dominant peak close to $k = 0$ is much smaller (see figure 2(c)).

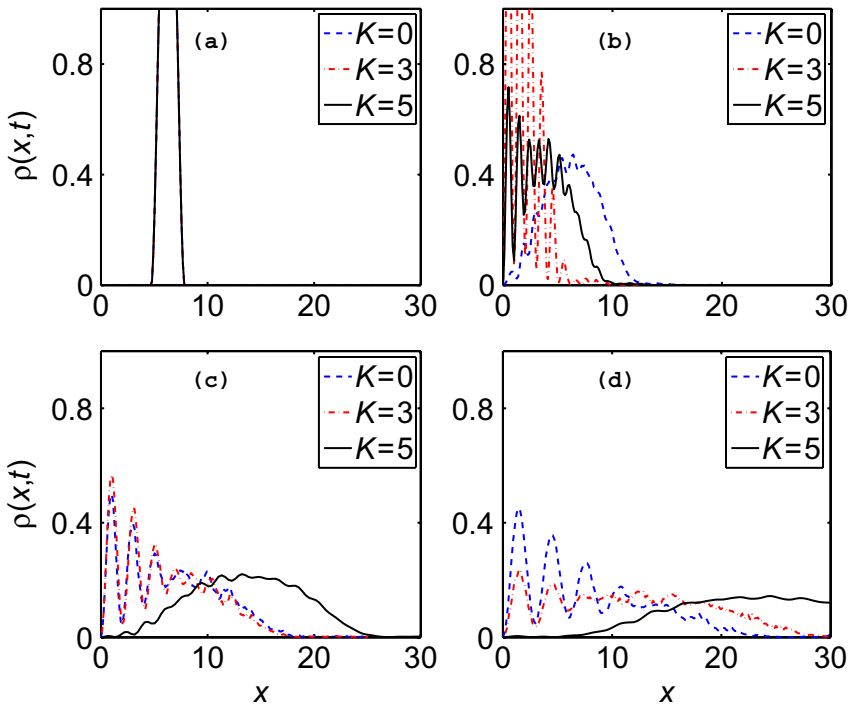

Figure 3. Density evolution of a Lieb–Liniger wave packet consisting of $N = 3$ bosons, which is given some momentum kick K (per particle) toward the wall. Insets correspond to the times (a) $t = 0$, (b) $t = 1$, (c) $t = 2$ and (d) $t = 3$. The interaction strength is $c = 1$. Blue dashed lines are for $K = 0$, red dot-dashed lines are for $K = 3$ and black solid lines are for $K = 5$.

Next, we explore dependence of the time evolution on the imparted momentum. To this end, we fix the interaction strength at $c = 1$, and observe the time-evolution for three different initial conditions (see figures 3 and 4): (i) expansion in the presence of the wall occurs when $K = 0$, (ii) reflection at an intermediate value $K = 3$ and (iii) for large value of the imparted momentum $K = 5$. The wave packets for $K = 3$ and 5 have the property that basically all of the initial momentum distribution is directed toward the wall, i.e. the distribution at $t = 0$ is on the negative k-axis. In contrast, exactly half of the initial momentum distribution of the wave packet for $K = 0$ is positive (negative). The basic distinction between these cases is that the wave packets with sufficiently large imparted momentum K get simply reflected from the wall and at larger times the interference fringes are almost negligible. For example, the wave packet with $K = 5$ is practically completely reflected from the wall at $t = 2$, see solid black lines in figures 3(c) and 4(c); the momentum distribution is on the positive k-axis and the interference fringes are essentially absent. In contrast, for $K = 0$ half of the momentum distribution is already positive (corresponding to motion away from the wall), and this part interferes with the reflected component at all times of the evolution. Note that the wave packet with $K = 0$ is still in the process of reflection from the wall at $t = 2$ because a large fraction of its momentum distribution is still on the negative k-axis, see dashed blue line in figure 4(c); the interference fringes are the largest in this case, see dashed blue line in figure 3(c).

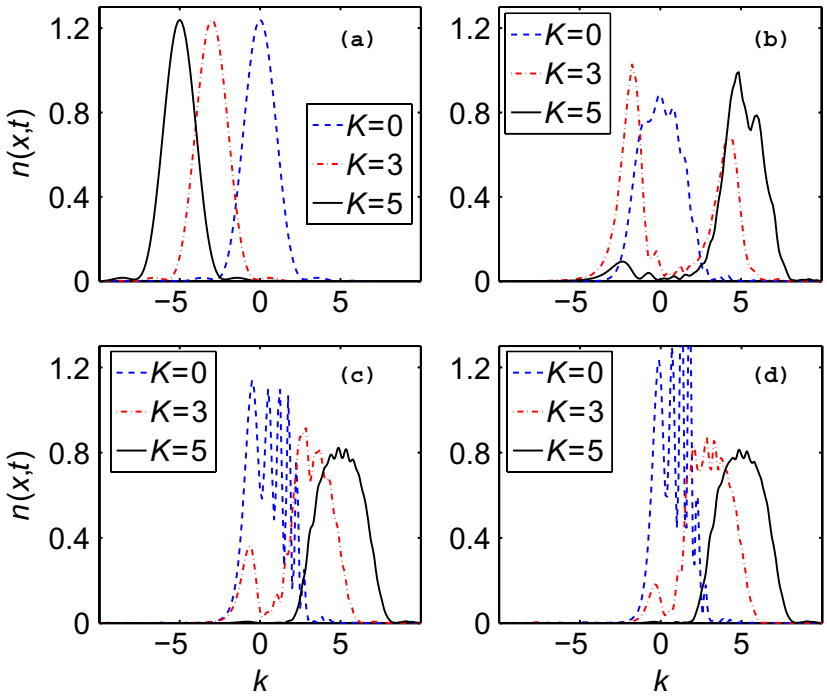

Figure 4. The same as figure 3 but for the momentum distribution.

Exact solutions can serve as a benchmark to check the range of validity of other methods, which may be used to analyze non-equilibrium dynamics of interacting systems. We have compared the solutions obtained with the Fourier transform method presented here with the so-called hydrodynamic formalism [10], which describes the Lieb–Liniger system via the nonlinear Schrödinger equation with variable nonlinearity [41]. In figures 5(a)–(d), we show density profiles for two different couplings ($c = 0.25$ and $c = 3$) at two different times ($t = 1$ and $t = 2$). We find that the SP density (and momentum distribution), calculated within this method, are in good agreement with our simulations for small values of the coupling parameter c (up to $c = 1$); this upper limit for c also depends on the initial density of the 1D Bose gas, as it is well known that the effective interaction strength parameter is c divided by the linear density [6]. However, for larger values of c, the hydrodynamic formalism goes beyond its range of validity for the simulations presented here. For example, for the simulations at intermediate interaction strength $c = 3$ (see figures 5(c) and (d)), the hydrodynamic formalism predicts deeper interference fringes than those obtained via the Fourier transform method; this is attributed to the fact that the hydrodynamic formalism overestimates the spatial coherence of the wave packet [10, 41]. For sufficiently large c, the system is in the TG regime, and one can employ the Fermi–Bose mapping [7, 35] to study the dynamics. In figures 5(e) and (f), we compare our calculation with that obtained via Fermi–Bose mapping ($c = \infty$, [7, 35]) for a large value of the interaction strength $c = 10$; we observe that qualitative features of the TG regime such as the N peaks in the initial SP density coincide with the two calculations; however, even larger c is needed to obtain better quantitative agreement.

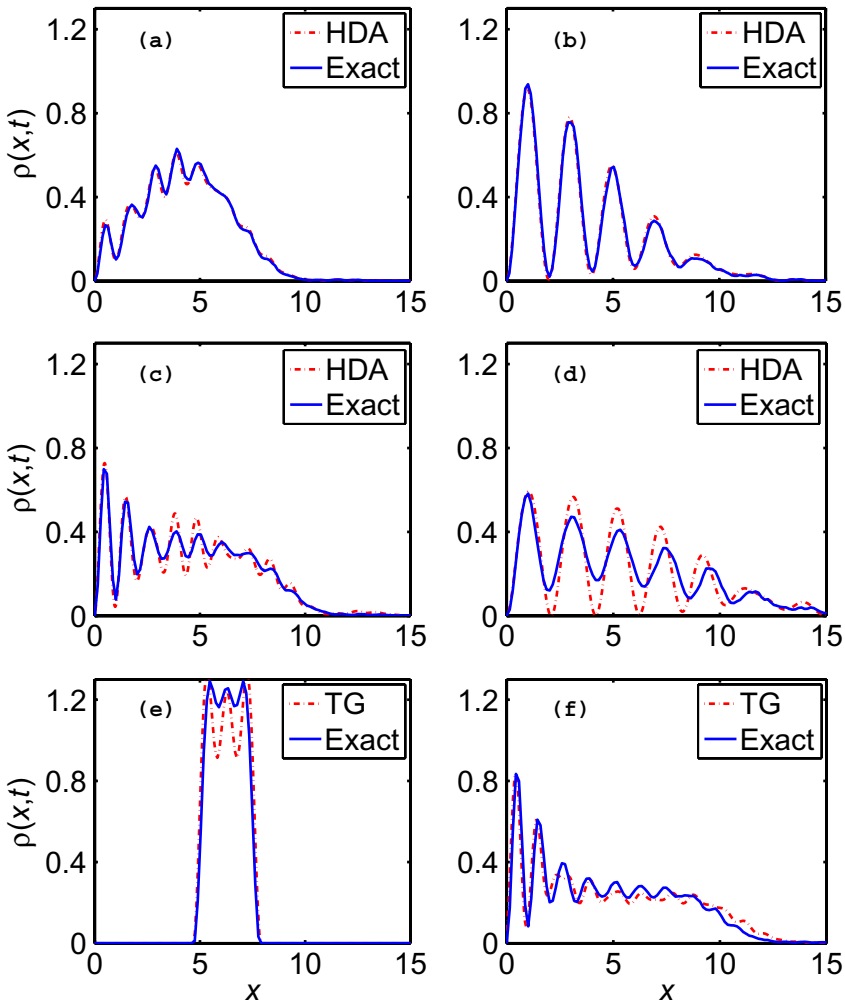

Figure 5. Comparison of the density evolution in the exact calculation, with the hydrodynamic approximation (HDA) (a)–(d), and the Fermi–Bose mapping (e) and (f) valid in the TG regime. The interaction strengths c and times t are (a) $c = 0.25$, $t = 1$, (b) $c = 0.25$, $t = 2$, (c) $c = 3$, $t = 1$, (d) $c = 3$, $t = 2$, (e) $c = 10$, $t = 0$ and (f) $c = 10$, $t = 1$. The initially imparted momentum is $K = 1$ for all figures.

4.1. Normalization of eigenstates

In order to numerically check our conjecture that the Lieb–Liniger hard-wall eigenstates defined in (5) are properly normalized, we have compared the initial state obtained via $\psi_{g.s.}(x_1, x_2, x_3)\exp[-\mathrm{i}K(x_1 + x_2 + x_3)]$, and the wave function obtained via equation (12) by employing the function $G(k_1, k_2, k_3)$, which is calculated from the projection coefficients $b(k_1, k_2, k_3)$ as in equation (13). We found that the relative agreement between the two wave functions is of the order of 1% or better, which is of the order of the numerical accuracy for the size of our numerical grid, which is limited by computer memory. We have performed this comparison for various initial conditions (different K and c values). Unfortunately, a rigorous proof of normalization of the Lieb–Liniger hard-wall eigenstates is, to the best of our knowledge, still lacking.

4.2. Connection to physical units

If we consider a system of ^{87}Rb atoms, then the ratio $X_0^2/T_0 \approx 3.65 \times 10^{-10}\,\mathrm{m^2\,s^{-1}}$ is fixed. By choosing, for example, $X_0 \approx 1.35\,\mu$m for the spatial scale, the temporal scale is set to $T_0 = 5$ ms. The 3D scattering length is $a = 5.3$ nm. The interaction parameter c can be varied by changing the width of transversal confinement $l_\perp$; for example, the values of $c = 0.25$ up to $c = 10$ can be obtained by varying $l_\perp$ from 242 nm down to $l_\perp \approx 41$ nm, respectively. Of course, for a different choice of temporal and spatial scales, transversal confinements $l_\perp$ would have different values. We have also verified that for the choice of scales in our example, the longitudinal energy E_0 is less than the transverse energy spacing $\hbar\omega_\perp$, a condition needed for freezing the radial degrees of freedom.

5. Conclusion

We have studied reflections of a Lieb–Liniger wave packet from the hard-wall potential. By employing the symmetry of the many-body eigenstates with respect to the change of the sign and permutation of their quantum numbers (i.e. quasi-momenta), that is, equations (9) and (10), we have demonstrated that the time evolution of this interacting many-body wave packet can be represented in terms of an N-dimensional Fourier transform, where N is the number of particles in the wave packet. This result simplifies our understanding of the time evolution in this many-body problem and enables straightforward calculation of the time-asymptotic properties of the system.

We have utilized the formalism to numerically study the dynamics of SP density and momentum distribution of a few-body wave packet reflecting from the wall (the wave packet is initially close to the wall). Reflection dynamics and interference phenomena depend on the strength of the interaction between the particles c and the imparted momentum K toward the wall. The wave packets for smaller c get reflected at a slower rate. Moreover, the interference fringes are deeper (larger visibility) for smaller values of c. If K is sufficiently large such that the initial momentum distribution is on the negative k-axis, the wave packet gets reflected and the interference fringes become small as soon as most of the momenta become positive. On the other hand, for $K = 0$, the interference effects are fairly large.

Acknowledgments

This work was supported by the Croatian Ministry of Science (grant no. 119-0000000-1015), the Croatian National Foundation for Science and the Croatian–Israeli Project Cooperation. We are grateful to Adolfo del Campo and Ofir Alon for useful comments and suggestions.

Appendix. The ground state of a Lieb–Liniger gas in an infinitely deep box

In section 4, we studied the Lieb–Liniger dynamics in the presence of the hard wall potential, with an example of three Lieb–Liniger bosons that are at $t < 0$ confined in the ground state of an infinitely deep box of length $L = \pi$. The ground state in fundamental permutation sector R_1 has been constructed by Gaudin [25] via a superposition of 2^N free space eigenstates. For the

box in the interval $[1.5\pi, 2.5\pi]$, the ground state (up to a normalization constant) reads

$$\psi_{g.s.}(x_1, \ldots, x_N) \propto \sum_{\{\epsilon\}} \epsilon_1 \cdots \epsilon_N \prod_{i<j} \left(1 - \frac{\mathrm{i}c}{q_i + q_j}\right) \sum_P \prod_{i<j} \left(1 + \frac{\mathrm{i}c}{q_{Pi} - q_{Pj}}\right) \times \exp\left(\mathrm{i} \sum_j q_{Pj}(x_j - 1.5\pi)\right). \tag{A.1}$$

Here, summations are taken over 2^N elements of set $\{\epsilon\}$, and $N!$ permutations P. The quasi-momenta $q_j = \epsilon_j |q_j|$, for $j = 1, \ldots, N$, are determined by the set of transcendental equations

$$|q_i| L = \pi + \sum_{j \neq i} \left(\tan^{-1} \frac{c}{|q_i| - |q_j|} + \tan^{-1} \frac{c}{|q_i| + |q_j|}\right). \tag{A.2}$$

Equation (A.2) is solved numerically. For the initial state corresponding to three particles ($N = 3$), where $\psi(x_1, x_2, x_3, t = 0) = \psi_{g.s.}(x_1, x_2, x_3)\exp[-\mathrm{i}K(x_1 + x_2 + x_3)]$, it is straightforward to obtain the projection coefficients $b(\{k\})$ by employing equation (8) and the orthonormality of eigenstates $\phi_{\{k\}}$.

References

[1] Schreck F, Khaykovich L, Corwin K L, Ferrari G, Bourdel T, Cubizolles J and Salomon C 2001 *Phys. Rev. Lett.* **87** 080403
Görlitz A *et al* 2001 *Phys. Rev. Lett.* **87** 130402
Greiner M, Bloch I, Mandel O, Hänsch T W and Esslinger T 2001 *Phys. Rev. Lett.* **87** 160405
Moritz H, Stöferle T, Kohl M and Esslinger T 2003 *Phys. Rev. Lett.* **91** 250402
Laburthe-Tolra B, O'Hara K M, Huckans J H, Phillips W D, Rolston S L and Porto J V 2004 *Phys. Rev. Lett.* **92** 190401
Stöferle T, Moritz H, Schori C, Kohl M and Esslinger T 2004 *Phys. Rev. Lett.* **92** 130403

[2] Kinoshita T, Wenger T and Weiss D S 2004 *Science* **305** 1125
Paredes B, Widera A, Murg V, Mandel O, Fölling S, Cirac I, Shlyapnikov G V, Hänsch T W and Bloch I 2004 *Nature* **429** 277

[3] Kinoshita T, Wenger T and Weiss D S 2006 *Nature* **440** 900

[4] Hofferberth S, Lesanovsky I, Fischer B, Schumm T and Schmiedmayer J 2007 *Nature* **449** 324

[5] van Amerongen A H, van Es J J P, Wicke P, Kheruntsyan K V and van Druten N J 2008 *Phys. Rev. Lett.* **100** 090402

[6] Lieb E and Liniger W 1963 *Phys. Rev.* **130** 1605
Lieb E 1963 *Phys. Rev.* **130** 1616

[7] Girardeau M 1960 *J. Math. Phys.* **1** 516

[8] Olshanii M 1998 *Phys. Rev. Lett.* **81** 938

[9] Petrov D S, Shlyapnikov G V and Walraven J T M 2000 *Phys. Rev. Lett.* **85** 3745

[10] Dunjko V, Lorent V and Olshanii M 2001 *Phys. Rev. Lett.* **86** 5413

[11] Rigol M, Dunjko V and Olshanii M 2008 *Nature* **452** 854

[12] Iglói F and Rieger H 2000 *Phys. Rev. Lett.* **85** 3233

[13] Sengupta K, Powell S and Sachdev S 2004 *Phys. Rev.* A **69** 053616

[14] Rigol M, Dunjko V, Yurovsky V and Olshanii M 2007 *Phys. Rev. Lett.* **98** 050405

[15] Cazalilla M 2006 *Phys. Rev. Lett.* **97** 156403

[16] Calabrese P and Cardy J 2006 *Phys. Rev. Lett.* **96** 136801

[17] Cherng R W and Levitov L S 2006 *Phys. Rev.* A **73** 043614
[18] Kollath C, Läuchli A M and Altman E 2007 *Phys. Rev. Lett.* **98** 180601
[19] Gaudin M 1983 *La fonction d'Onde de Bethe* (Paris: Masson)
[20] Girardeau M D 2003 *Phys. Rev. Lett.* **91** 040401
[21] Buljan H, Pezer R and Gasenzer T 2008 *Phys. Rev. Lett.* **100** 080406
see also Buljan H, Pezer R and Gasenzer T 2009 *Phys. Rev. Lett.* **102** 049903
[22] Jukić D, Pezer R, Gasenzer T and Buljan H 2008 *Phys. Rev.* A **78** 053602
[23] Jukić D, Klajn B and Buljan H 2008 *Phys. Rev.* A **79** 033612
[24] Gritsev V, Rostunov T and Demler E 2009 arXiv:0904.3221v2
[25] Gaudin M 1971 *Phys. Rev.* A **4** 386
[26] Busch T, Englert B-G, Rzazewski K and Wilkens M 1998 *Found. Phys.* **28** 4
[27] Muga J G and Snider R F 1998 *Phys. Rev.* A **57** 3317
[28] Sakmann K, Streltsov A I, Alon O E and Cederbaum L S 2005 *Phys. Rev.* A **72** 033613
[29] Batchelor M T, Guan X-W, Oelkers N and Lee C 2005 *J. Phys. A: Math. Gen.* **38** 7787
[30] Hao Y, Zhang Y, Liang J Q and Chen S 2006 *Phys. Rev.* A **73** 063617
[31] Sykes A G, Drummond P D and Davis M J 2007 *Phys. Rev.* A **76** 063620
[32] Kanamoto R, Carr L D and Ueda M 2009 arXiv:0910.2805v1 [cond-mat.quant-gas]
[33] Korepin V E, Bogoliubov N M and Izergin A G 1993 *Quantum Inverse Scattering Method and Correlation Functions* (Cambridge: Cambridge University Press)
[34] Gaudin M 1971 *J. Math. Phys.* **12** 1677
Gaudin M 1971 *J. Math. Phys.* **12** 1674
[35] Girardeau M D and Wright E M 2000 *Phys. Rev. Lett.* **84** 5691
[36] Rigol M and Muramatsu A 2005 *Phys. Rev. Lett.* **94** 240403
Rigol M and Muramatsu A 2005 *Mod. Phys. Lett.* B **19** 861
[37] Pezer R and Buljan H 2007 *Phys. Rev. Lett.* **98** 240403
[38] Minguzzi A and Gangardt D M 2005 *Phys. Rev. Lett.* **94** 240404
[39] del Campo A and Muga J G 2006 *Europhys. Lett.* **74** 965
[40] Gangardt D M and Pustilnik M 2008 *Phys. Rev.* A **77** 041604
[41] Öhberg P and Santos L 2002 *Phys. Rev. Lett.* **89** 240402
Pedri P, Santos L, Öhberg P and Stringari S 2003 *Phys. Rev.* A **68** 043601
[42] Vidal G 2004 *Phys. Rev. Lett.* **93** 040502
[43] Muth D, Schmidt B and Fleischhauer M 2009 arXiv:0910.1749v1 [quant-ph]
[44] Rey A M, Hu B L, Calzetta E, Roura A and Clark C W 2004 *Phys. Rev.* A **69** 033610
[45] Gasenzer T, Berges J, Schmidt M G and Seco M 2005 *Phys. Rev.* A **72** 063604
Berges J and Gasenzer T 2007 *Phys. Rev.* A **76** 033604
[46] Alon O E, Streltsov A I and Cederbaum L S 2008 *Phys. Rev.* A **77** 033613
[47] Zöllner S, Meyer H-D and Schmelcher P 2008 *Phys. Rev.* A **78** 013621
[48] Caux J-S, Calabrese P and Slavnov N A 2007 *J. Stat. Mech.* P01008
[49] Bloch I, Dalibard J and Zwerger W 2008 *Rev. Mod. Phys.* **80** 885
[50] del Campo A, Garcia-Calderon G and Muga J G 2009 *Phys. Rep.* **476** 1
[51] Pezer R, Gasenzer T and Buljan H 2009 *Phys. Rev.* A **80** 053616
[52] Wang Y-J, Anderson D Z, Bright V M, Cornell E A, Diot Q, Kishimoto T, Prentiss M, Saravanan R A, Segal S R and Wu S 2005 *Phys. Rev. Lett.* **94** 090405
[53] Bongs K, Burger S, Birkl G, Sengstock K, Ertmer W, Rzazewski K, Sanpera A and Lewenstein M 1999 *Phys. Rev. Lett.* **83** 3577
[54] Steyerl A *et al* 1986 *Phys. Lett.* A **116** 347
[55] Libson A, Riedel M, Bronshtein G, Narevicius E, Even U and Raizen M G 2006 *New J. Phys.* **8** 77
[56] Narevicius E, Libson A, Riedel M F, Parthey C G, Chavez I, Even U and Raizen M G 2007 *Phys. Rev. Lett.* **98** 103201
[57] Reinaudi G, Wang Z, Couvert A, Lahaye T and Guéry-Odelin D 2006 *Eur. Phys. J.* D **40** 405